

## Energy and evapotranspiration partitioning in a desert vineyard



D. Kool<sup>a,b</sup>, W.P. Kustas<sup>c</sup>, A. Ben-Gal<sup>b</sup>, N. Lazarovitch<sup>a</sup>, J.L. Heitman<sup>d</sup>, T.J. Sauer<sup>e</sup>,  
N. Agam<sup>a,\*</sup>

<sup>a</sup> Jacob Blaustein Institutes for Desert Research, Ben-Gurion University of the Negev, Sede Boqer Campus, Be'er Sheva 84990, Israel

<sup>b</sup> Institute of Soil, Water and Environmental Sciences, Agricultural Research Organization, Gilat Research Center, Mobile Post Negev 2, Gilat 85280, Israel

<sup>c</sup> USDA-ARS Hydrology and Remote Sensing Laboratory, Bldg. 007, Rm. 104, Beltsville, MD 20705, USA

<sup>d</sup> Soil Science Department, North Carolina State University Raleigh, Raleigh, NC 27695, USA

<sup>e</sup> National Laboratory for Agriculture and Environment, USDA-ARS, Ames, IA 50011, USA

### ARTICLE INFO

#### Article history:

Received 29 June 2015

Received in revised form 5 January 2016

Accepted 5 January 2016

#### Keywords:

Evaporation

Transpiration

Latent heat

Sparse canopy

Water use efficiency

Energy balance

Water balance

Crop coefficient

### ABSTRACT

The challenge of partitioning energy and evapotranspiration ( $ET$ ) components was addressed over a season (bud break till harvest) in a wine grape vineyard located in an extreme arid region. A below canopy energy balance approach was applied to continuously estimate evaporation from the soil ( $E$ ) while system  $ET$  was measured using eddy covariance. Below canopy energy balance was assessed at the dry midrow position as well as the wet irrigated position directly underneath the vine row, with  $E$  calculated as the residual of measured net radiation, soil heat flux, and computed sensible heat flux. The variables used to compute sensible heat flux included soil surface temperature measured using infrared thermometers and below-canopy wind speed in a soil resistance formulation that required a modified wind factor. The  $E$  derived from below canopy energy balance was reasonable at daily intervals although it underestimated micro-lysimeter  $E$  measurements, suggesting there may have been advected energy from the midrow to the below-vine position. Seasonal partitioning indicated that total  $E$  amounted to 9–11% of  $ET$ . In addition, empirical functions from the literature relating crop coefficients ( $K_{cb}$ ) to plant size, appeared to give reasonable results under full canopy, albeit with some day to day variation, but underestimated  $K_{cb}$  during the growing period.

© 2016 Published by Elsevier B.V.

### 1. Introduction

Partitioning of energy and water fluxes in vegetated systems can give valuable information on the productive use of water through plant transpiration ( $T$ ) and losses due to evaporation from the soil ( $E$ ), which is generally considered an unproductive form of water use. This is relevant for food production, ecosystem functioning, and climate; particularly in the light of increasing water scarcity and drought as a result of anthropogenic activity and projected climate change. In arid areas,  $E$  is potentially substantial due to high evapotranspiration ( $ET$ ) dominating the water balance and the prevalence of sparse vegetation (Wilcox et al., 2003). As  $E$  and  $T$  differ in their response to environmental conditions, separate assessment is necessary to adequately determine ecosystem energy and water exchange under different weather and climate conditions (Kool et al., 2014a; Lawrence et al., 2007; Zhang et al., 2011).

For many agricultural row crops, determining  $E$  and  $T$  is critical for assessing water use efficiency. This is particularly true for grapevines which are one of the world's most economically important horticultural crops (Williams and Ayars, 2005) and are increasingly grown in arid regions (Li et al., 2009; Sene, 1994). Wine grape vineyards are generally characterized by relatively small canopy cover fractions designed to optimize grape cluster micro-climate and radiation availability (Pieri, 2010a). While vineyards are traditionally rain-fed, irrigated viticulture is becoming increasingly common (Ortega-Farías et al., 2010). Water supply strongly affects grape yield quantity and wine quality (Trambouze et al., 1998), where mild stress can improve quality but severe stress can result in reduced quality (Van Leeuwen et al., 2009) and, in severe cases, plant death. Optimal grape production therefore requires precise water management, which is expected to benefit from understanding of energy and water partitioning within the vineyard.

Knowledge of vineyard water status is required to understand mechanisms of vegetative versus reproductive growth (Shapland et al., 2012; Van Leeuwen et al., 2009), short and long-term effects of deficit irrigation (Zhang et al., 2011), and how drought stress

\* Corresponding author. Tel.: +972 8 6563471.  
E-mail address: [agam@bgu.ac.il](mailto:agam@bgu.ac.il) (N. Agam).

affects specific stages in vine phenology and grape ripening (Van Leeuwen et al., 2009). Crop coefficients ( $K_c$ ) which relate vineyard water requirements to atmospheric demand have been developed to determine optimal irrigation strategies, plant water status and severity of drought stress. Since vineyard  $K_c$  varies widely depending on vine training practices, plant cover, and grape variety and rootstock,  $K_c$  is often determined separately for plant ( $K_{cb}$ ) and soil surface ( $K_e$ ) components (Allen et al., 1998). In addition, efforts have been made to relate  $K_{cb}$  to plant canopy parameters such as leaf area index (LAI) or ground fraction cover (Ferreira et al., 2012; Netzer et al., 2009; Picón-Toro et al., 2012; Poblete-Echeverría and Ortega-Farías, 2009; Williams and Ayars, 2005). In order to obtain accurate water requirement parameters including  $K_c$  and  $K_{cb}$ , assessment of seasonal  $ET$  and its partitioning are of importance. Continuous assessment of  $T$  has been reasonably successful using sapflow or chamber measurements, though major challenges remain (Wullschlegel et al., 1998). In contrast, continuous measurements of  $E$  are basically non-existent (Kerridge et al., 2013; Kool et al., 2014a).

The partitioning of vineyard energy balance components between the soil and the canopy is not easily predicted, although it is known that the soil contribution to system fluxes is considerable (Ortega-Farías et al., 2010; Sene, 1994; Spano et al., 2000). For example, there is evidence that soil sensible heat contributes to canopy  $T$ , (Heilman et al., 1994; Hicks, 1973) and may also contribute available radiation to berry clusters (Pieri, 2010a, 2010b). Available energy is also affected by surface shading which is not uniform across the inter-row (Horton, 1989; Horton et al., 1984; Pieri, 2010a). An additional unknown is how energy partitioning is regulated in drip-irrigated systems, where wet soil near the dripper and bare strips between vine rows have to be considered separately (Kool et al., 2014b; Poblete-Echeverría and Ortega-Farías, 2009). In addition, important micro-climate variables, such as below canopy wind speed in widely spaced vineyards with relatively sparse vegetation, are not yet well understood (Poblete-Echeverría and Ortega-Farías, 2009).

Modeling of sparse-canopy crops often relies on energy balance to describe system water use. Such modeling requires a good understanding of the complex interaction between vine, soil and atmospheric conditions (Colaizzi et al., 2012; Ding et al., 2015; Ortega-Farías et al., 2010; Poblete-Echeverría and Ortega-Farías, 2009). While studies regarding water requirements tend to focus on seasonal data (Ferreira et al., 2012; Yunusa et al., 2004; Zhang et al., 2011), detailed studies regarding canopy energy balance and interactions between soil and vine components have generally been conducted for only brief periods under well-watered conditions and full canopy cover (Heilman et al., 1994; Li et al., 2009; Pieri, 2010a; Sene, 1994). The assessment of energy partitioning at a seasonal scale, taking into account variability across the soil surface as well as between the surface and the canopy, is a novel aspect of the current approach. The objectives of this research were: to study the effects of canopy growth, irrigation, and changes in atmospheric conditions on energy partitioning; to assess productive and unproductive allocation of water through  $ET$  partitioning and; to determine the utility of the below canopy energy balance approach toward obtaining continuous estimation of  $E$ .

## 2. Methods

### 2.1. Site description

A field experiment was conducted in a ~10 ha drip-irrigated commercial vineyard in the arid central Negev highlands, Israel (30.7°N, 34.8°E, altitude 550 m) from bud break until harvest during the growing season of 2012. Vineyard row orientation was

approximately north-south, with 3 m distance between rows. The vines were planted 1.5 m apart and were trained on a vertical-shoot-positioned system, with 1 m cordon height and vines attaining a maximum height of ~1.8 m. The 10-year-old Cabernet Sauvignon (*Vitis vinifera* L., on 140 Ruggeri rootstock) vineyard formed an isolated irrigated area in a dry bare surrounding on level terrain. Long-term average daily temperature minima and maxima for the region range from 4.4 to 14.8 °C in January and 18.1 to 32.7 °C in July. During the early growing season, temperatures range between 10.5 and 25.1 (April), 13.5 and 28.7 (May) and 16 and 31.2 (June). Precipitation at the site is erratic and mostly occurs between November and April, averaging <100 mm y<sup>-1</sup> (Israel Meteorological Service). In the winter prior to the 2012 growing season a total of 48.3 mm rainfall was recorded with the last rain event in the spring consisting of 2.5 mm on 16 March. The growing season started with bud break on 1 April 2012 and continued through July without a single rain event.

### 2.2. Measurement set-up

A detailed description of the experimental set-up as well as the site meteorological conditions is reported in Kool et al. (2014b). In brief, standard meteorological measurements included solar radiation, air temperature and humidity, precipitation, and wind speed and direction. Other measurements included irrigation amounts and hourly measurements of  $E$  using micro-lysimeters (MLs) during three 24-h intensive observation periods (IOPs). In brief, the MLs were 100 mm deep, had a diameter of 110 mm and were made of PVC. The MLs were pushed into the soil, excavated, capped to prevent losses other than evaporation, weighed and placed in a preformed hole with the same position relative to the vine-row as the original sample location. The installed MLs were removed and weighed hourly ( $\pm 0.1 \text{ g} \approx 0.011 \text{ mm}$ ) from pre-dawn to after sunset. The LAI was measured using an LAI-2000 (Li-Cor Bioscience Inc., Lincoln, NE<sup>1</sup>) following recommendations for row crops. Plant canopy height and width were measured during each site visit, about once a week. Surface temperatures were measured using four infrared radiometers (IRTS-P, field-of-view 28° half angle, Apogee Instruments Inc., Logan, UT). The composite (system) temperature was assessed by two IRTs deployed at the top of a 7 m tall arch, positioned directly above the vine row and midrow, respectively. The other two IRTs were positioned with their field-of-view directly below the vine at 0.3 m height, and above the midrow at 2.5 m height. Air temperature was measured at 3.3 m above the soil surface (HMP45C, Vaisala Inc., Woburn, MA and 10-Plate Gill Radiation Shield, R.M. Young, Traverse City, MI) and directly below the vine at 0.06 m height, where air was drawn to a shielded Beta-Therm thermistor through a 4.3 mm-i.d. rigid metal/plastic composite tube (Synflex Type 1300, Eaton Synflex, Mantua, OH) using a 12 VDC pump (NMP 830, KNF Neuberger Inc., Trenton, NJ) and rotameter (PMR1-01065S, Cole Parmer, Vernon Hills, IL) to control the flow rate (<1 L min<sup>-1</sup>). Data were logged at 10 s intervals, and 15 min averages were stored using CR23X and CR5000 dataloggers (Campbell Scientific Inc., Logan, UT). Hourly reference  $ET_0$  was calculated using solar radiation, wind speed, air temperature, and humidity at 2 m height data from a nearby weather station, following the FAO Penman–Monteith model (Allen et al., 1998; Kool et al., 2014b).

<sup>1</sup> The use of trade, firm, or corporation names in this article is for the information and convenience of the reader. Such use does not constitute an official endorsement or approval by the United States Department of Agriculture or the Agricultural Research Service of any product or service to the exclusion of others that may be suitable.

Energy balance components were assessed at system level and below the canopy near the soil surface (subscript *s*) in the midrow (MR) and directly below the vine (BV). System net radiation ( $R_n$ ) was measured at 5 m height, while  $R_n$  below the canopy,  $R_{ns,MR}$  and  $R_{ns,BV}$ , was measured at 0.3 m height (Q\*7, Radiation and Energy Balance Systems, Seattle, WA). Soil heat flux ( $G$ ) was measured at five positions, two midrow positions, two positions at 0.3 m to either side of the vine row, and one position directly under the vine row. Measurements were conducted using flux plates (HFT1.1, Radiation and Energy Balance Systems, Seattle, WA) at 0.06 m depth. Heat storage above the plates was accounted for using IRT surface temperature measurements and thermocouples at depths of 0.015, 0.045, and 0.06 m, adjacent to each plate, in addition to water content sensors (SDI-12 Soil Moisture Transducer, Acclima Inc., Meridian, ID) to determine heat capacity, also at 0.06 m depth adjacent to each plate (Sauer, 2002). To ensure that  $G$  and  $R_{ns}$  measurement positions were similar, an average of the two  $G$  measurements in the midrow was chosen to represent  $G_{MR}$ , while the  $G$  measurement under the vine row was chosen to represent  $G_{BV}$ . System  $G$  was taken as a weighted average of  $G_{MR}$  and  $G_{BV}$ . Data were logged at 10 s intervals, and 15 min averages were stored using CR23X dataloggers (Campbell Scientific Inc., Logan, UT).

System  $ET$  and sensible heat ( $H$ ) fluxes were determined using an eddy covariance system (CSAT 3-D sonic anemometer, Campbell Scientific Inc., Logan, UT; with an open path infrared gas analyzer, LI-7500, Li-Cor Biosciences Inc., Lincoln, NE) mounted 3.3 m above the soil surface, facing the predominant wind direction (NW). Data were recorded at 10 Hz using a CR5000 data logger (Campbell Scientific Inc., Logan, UT). Alongside the eddy covariance system additional measurements of water vapor density (HMP45C, Vaisala Inc., Woburn, MA enclosed in a 10-Plate Gill Radiation Shield, R.M. Young, Traverse City, MI) were logged at 10 s intervals, and stored every 15 min using the same CR5000 data logger. Errors in vapor fluxes that ensued from accumulation of dust on the sensor head were corrected by calibrating raw high frequency vapor concentrations to HMP water vapor densities following Fratini et al. (2014). Post processing of the eddy covariance data included de-spiking according to the algorithm developed by Goring and Nikora (2002), correction for humidity and crosswind effects on sonic temperature (Liu et al., 2001; Schotanus et al., 1983), 2-D coordinate rotation correction (Tanner and Thurtell, 1969), frequency response correction (Massman, 2000), and the correction for buoyancy effects described by Webb et al. (1980). Corrected sensible and latent heat fluxes were calculated on a half-hourly basis. Note that energy used for fixation of carbon dioxide and heat storage in the canopy layer was considered negligible.

### 2.3. Below canopy energy balance computations

Below the canopy,  $E$  fluxes were assumed to be limited to the strip directly below the vine where the drip line was located (discussed further in Section 2.4).  $E$  was computed as a residual of the energy balance equation:

$$\lambda E = R_{ns,BV} - G_{BV} - H_{s,BV} \quad (1)$$

where  $\lambda$  is latent heat of vaporization ( $\text{J kg}^{-1}$ ) and energy fluxes are in  $\text{W m}^{-2}$ . This notation defines  $R_n$  as positive toward the surface and  $\lambda E$ ,  $H$ , and  $G$ , as positive away from the surface. Assuming zero  $E$  in the midrow, the midrow energy balance could be defined as

$$H_{s,MR} = R_{ns,MR} - G_{MR} \quad (2)$$

Midrow and below-vine  $H_s$ ,  $H_{s,BV}$  and  $H_{s,MR}$ , can be computed using:

$$H_{s,BV} = \rho c_p \frac{T_{s,BV} - T_{a,BV}}{r_{as,BV}} \quad (3a)$$

$$H_{s,MR} = \rho c_p \frac{T_{s,MR} - T_{a,MR}}{r_{as,MR}} \quad (3b)$$

where  $\rho$  ( $\text{kg m}^{-3}$ ) and  $c_p$  ( $\text{J kg}^{-1} \text{K}^{-1}$ ) are the density and specific heat of air, respectively,  $T_s$  (K) is measured soil surface temperature,  $T_{a,BV}$  (K) is measured air temperature below the vine,  $T_{a,MR}$  (K) is estimated air temperature in the midrow, and  $r_{as}$  ( $\text{s m}^{-1}$ ) is resistance to heat transfer between the soil surface and the below-canopy air temperature reference height. Following Kustas and Norman (1999)  $r_{as}$  was calculated as

$$r_{as} = \frac{1}{c(T_s - T_a)^{1/3} + bu_s} \quad (4)$$

where  $c = 0.0025$ ,  $b = 0.012$ ,  $u_s$  ( $\text{m s}^{-1}$ ) is below canopy wind speed, and  $T_a$  (K) is mean below-canopy air temperature where  $T_s = T_{s,BV}$  and  $T_a = T_{a,BV}$  for  $r_{as,BV}$  and  $T_s = T_{s,MR}$  and  $T_a = T_{a,MR}$  for  $r_{as,MR}$ . For  $[(T_s - T_a) < 0]$ ,  $[c(T_s - T_a)^{1/3}]$  was replaced by constant  $a = 0.004$  (Kustas and Norman, 1999).

As has been reported elsewhere (e.g., Castellví and Snyder, 2009; Hicks, 1973; Raupach, 1992; Riou et al., 1987) traditional equations describing air flow in canopies are less applicable in the unique architecture that characterizes vineyards: a strongly clumped row crop with a large gap between the soil surface and the bottom of the canopy, which comprises 50% or more of the canopy height. Consequently, the underlying assumptions regarding the values of zero plane displacement ( $d$ ), roughness length ( $z_0$ ), the mean drag coefficient for individual leaves ( $c_d$ ), and extinction factor for wind ( $\gamma$ ) based on plant height, density and/or fractional cover/leaf area are tenuous. Furthermore the shape of the in-canopy wind profile may not be logarithmic but S-shaped, with secondary wind maxima below the plant canopy (Shaw, 1977). The authors are not aware of formulations that consider both strongly clumped canopy structure with leaf area concentrated in only a fraction of the canopy height (e.g., leaf area concentrated in the upper half of the canopy height) for estimating below canopy wind speed profiles. Therefore, to account for the unique vineyard architecture an empirical correction factor " $F_{VA}$ " to the estimated wind speed near the soil surface was introduced into the aerodynamic resistance formulation in order to compute reliable heat fluxes using Eqs. (3a) and (3b). The modified equation for  $r_{as}$  was defined as:

$$r_{as} = \frac{1}{c(T_s - T_a)^{1/3} + F_{VA}bu_s} \quad (5)$$

where  $u_s$  calculated using equations for continuous canopies. To determine  $F_{VA}$ ,  $H_{MR}$  was first computed as the residual of the midrow energy balance, using Eq. (2). Daily values for  $F_{VA}$  were obtained by optimization where daily sums of  $H_{MR}$  computed by Eq. (3b) were optimized to match  $H_{MR}$  using Eq. (2). Other soil resistance formulations were also employed and are discussed later, but, even with calibration, no other formulation could provide as reliable and consistent results as with Eq. (5). Similar to Norman et al. (1995),  $u_s$  was calculated using the following equations (Goudriaan, 1977):

$$u_s = u_c \exp \left[ -\gamma \left( \frac{1 - 0.15}{h_c} \right) \right] \quad (6)$$

$$u_c = u_z \left[ \frac{\ln((h_c - d)/z_0)}{\ln((z - d)/z_0) - \psi_M} \right] \quad (7)$$

$$\gamma = h_c^{1/3} s^{-1/3} 0.28 \Omega \text{LAI}^{2/3} \quad (8)$$

where  $u_c$  ( $\text{m s}^{-1}$ ) is wind speed at the top of the canopy,  $\gamma$  is unitless,  $h_c$  (m) is canopy height,  $d$  and  $z_0$  are in m,  $\psi_M$  (–) is the diabatic correction for momentum at the canopy height, which was assumed negligible due to sublayer roughness effects, and the mean size of individual leaves  $s$  (m), defined as the width of an equivalent square,

was computed as four times the leaf area divided by the perimeter. As LAI measurements represented a strongly clumped canopy, the effective LAI was calculated by multiplying measured LAI by a clumping factor  $\Omega$  (–), calculated as (Kustas and Norman, 1999)

$$\Omega = \ln \frac{[(1 - f_{veg})] + \exp(-0.5 \text{ LAI}/f_{veg}) f_{veg}}{-0.5 \text{ LAI}} \quad (9)$$

where the vegetated fraction ( $f_{veg}$ ) was determined as the vine width divided by the row width. The roughness parameters  $z_0$  and  $d$  were estimated using the formulations of Shaw and Pereira (1982) and Choudhury and Monteith (1988):

$$d = 1.1 h_c \ln \left[ 1 + (c_d \Omega \text{ LAI})^{1/4} \right] \quad (10)$$

$$z_0 = z'_0 + 0.3 h_c (c_d \Omega \text{ LAI})^{1/2} \quad (\text{for } c_d \Omega \text{ LAI} < 0.2) \quad (11)$$

where  $z'_0$  (0.005 m) is the roughness length of the soil substrate and  $c_d$  (–) was found to equal 0.07 in sparse canopies (Shuttleworth, 1991).

The maximum gradient between  $T_{s,MR}$  and  $T_{a,MR}$  can be derived from the formulation for the composite soil sensible heat flux ( $H_s$ ), which, considering interaction between vegetation and soil fluxes, is defined as

$$H_s = \rho c_p \frac{T_s - T_{ac}}{r_{as}} \quad (12)$$

where  $T_{ac}$  (K) is air temperature at a reference height in the canopy air space. Using eddy covariance measured  $H$ ,  $u_z$  and  $u^*$ ,  $T_{ac}$  was computed as

$$T_{ac} = T_a + \frac{H r_a}{\rho c_p} \quad (13)$$

and

$$r_a = \frac{u_z}{(u^*)^2} \quad (14)$$

where  $T_a$  (K) is measured temperature at height  $z$  (m),  $r_a$  ( $\text{m s}^{-1}$ ) is aerodynamic resistance to heat transfer between the canopy and above-canopy air temperature reference heights,  $u_z$  ( $\text{m s}^{-1}$ ) is wind speed above the canopy at height  $z$ , and  $u^*$  ( $\text{m s}^{-1}$ ) is friction velocity. However  $T_{a,MR}$  is likely to actually fall between  $T_{ac}$  and  $T_{s,MR}$  values and it can be defined as  $[(1-x)T_{ac} + xT_{s,MR}]$ , where  $x$  is a weighting factor of the two temperatures having a value between 0 and 1. Furthermore, in the optimization of Eqs. (2) and (3b) the wind speed below the canopy cannot exceed the wind speed right above the canopy, i.e.,  $F_{VA} u_s < u_c$ . Allowing for some uncertainty in  $u_c$ , it was found that for  $x = 0.3 F_{VA} u_s$  never exceeded  $u_c$  by more than 10%. It was therefore assumed that  $[0 < x < 0.3]$ , so taking the midpoint for  $x$  between 0 and 0.3, the average estimated  $T_{a,MR}$  was computed as  $[(1 - 0.15)T_{ac} + 0.15 T_{s,MR}]$ .

#### 2.4. Partial contribution of the midrow and below-vine positions

To determine the relative contribution of the below and midrow positions to total below canopy fluxes, it was imperative to establish the average width of the wet zone below the vine. As the wet zone was maintained by irrigation throughout the season, the width was assumed to be essentially constant. The percentage of the wet zone as seen by the IRT directly below the vine, and the dry zone as seen by the IRT in the midrow was assessed pre-bud break, when shading was negligible and temperature differences were largely dictated by differences in water content. The temperatures measured by IRTs at the two locations were compared to system IRT measurements ( $T_{system}$ ), the average of two IRTs set at 7 m above the ground where the field of view included both the vine and the inter-row; Fig. 1) over a two week period pre-season when the midrow was dry (>2 weeks after a rain event). As the

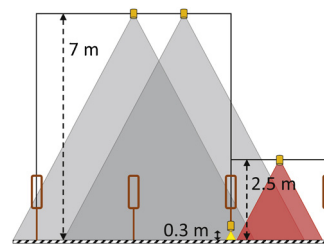


Fig. 1. Schematic representation of infrared thermometers' fields of view.

canopy had not yet developed, the IRTs positioned at 7 m gave the composite temperature of the soil surface, including both the dry midrow and the irrigated below-vine positions. Optimization for the relative width of the wet strip  $w$ , using least square regression where  $T_{system} = [w \times T_{s,BV}^4 + (1 - w) \times T_{s,MR}^4]^{1/4}$ , suggested that the midrow IRT represented 86% of the system and the below-vine IRT represented 14% of the system with a coefficient of determination ( $R^2$ ) of 1 relative to the 1:1 line.

### 3. Results

#### 3.1. Weather conditions

Meteorological data necessary to compute  $H$  and  $\lambda E$  fluxes included below canopy wind speed and temperature gradients are described below. Other weather conditions were described in detail by Kool et al. (2014b).

##### 3.1.1. Wind

Seasonal wind speeds were somewhat erratic at the beginning of the season changing to an almost invariable pattern toward the end of May. Strong winds reaching between 8 and 10  $\text{m s}^{-1}$  were observed in April, while from May until August winds typically reached around 4  $\text{m s}^{-1}$  in the late afternoons. LAI increased sharply from the end of April and halfway into May after which it stabilized. Peak LAI values reached 1.71, while  $f_{veg}$  reached 0.17, and  $\Omega \text{ LAI}$  reached 0.33. The value of the empirical factor  $F_{VA}$  was fairly uniform throughout the season, averaging 0.59 with a standard deviation of 0.16. Assessment of the influence of wind direction on  $F_{VA}$  indicated little difference between wind coming from perpendicular, parallel or 45° angle directions relative to the vine row orientation (data not shown).

##### 3.1.2. Temperatures

Surface temperatures across the inter-row were strongly affected by water content and shading at any given time throughout the season. An impression of the contrast in surface temperature at different times of a summer day (Fig. 2) reveals that in the morning and in the afternoon, when the wet area near the drippers was sunlit, the temperature was more than 10 °C lower in the wet sunlit area relative to a sunlit area in the dry midrow. Shaded wet and dry areas differed by as much as 6 °C. The contrast between shaded and sunlit dry areas reached almost 30 °C at noon and close to 20 °C a few hours before and after noon, where both sunlit and shaded areas were several degrees warmer in the afternoon as compared to the morning. Around solar noon (12:35), the instantaneous difference between a wet shaded point and a dry sunlit point was as high as 33 °C.

Seasonal assessment indicated that average daily surface temperatures at midrow and below-vine positions differed by 3.0 °C on irrigated days and 1.5 °C on non-irrigated days. Differences between midrow  $T_{s,MR}$  and  $T_{a,MR}$  peaked at around 18 °C at noon, showing similar patterns throughout the season (Fig. 3a). Below-vine  $T_{s,BV}$  and  $T_{a,BV}$  were strongly influenced by noon shading, with

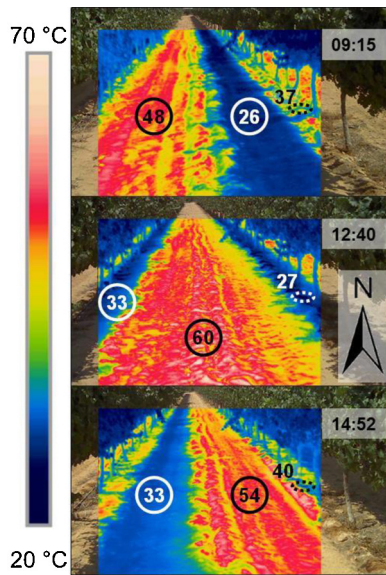


**Fig. 2.** RGB images with overlaid simultaneously acquired thermal images of the vineyard inter-row for 24 July, 2012. Circles center on shaded dry (white solid line circles) and sunlit dry (black solid line circles) areas, where the number represents the average surface temperature ( $^{\circ}\text{C}$ ). A dashed line circle was centered on a wetted area near a dripper, which was sometimes sunlit (black dashed line circles) and sometimes shaded (white dashed line circle).

$T_{s,BV}$  peaking around 9:30 and 14:00 and  $T_{a,BV}$  about 45 min later, both in the morning and in the afternoon. At both positions, the peaks in  $[T_s - T_a]$  coincided with peaks in  $T_s$  mentioned above, as shown in Fig. 3b and c. While  $T_s$  and  $T_a$  at both positions increased by about  $8^{\circ}\text{C}$  between April and July, seasonal changes in  $[T_s - T_a]$  were very minimal.

### 3.2. Energy balance assessment

#### 3.2.1. System energy balance closure

At the system level all energy balance components were measured independently. Energy balance closure was evaluated by linear regression of turbulent fluxes,  $H$  and  $\lambda ET$ , against available energy  $R_n$  and  $G$  (Fig. 4). The slope was 0.91, indicating that  $H$  and  $\lambda ET$  underestimated  $R_n$  and  $G$ . The intercept was  $-4.1 \text{ W m}^{-2}$  and  $R^2$  was 0.96. The energy balance ratio, defined as the sum of turbulent fluxes divided by the sum of available energy (Wilson et al., 2002), amounted to 0.88.

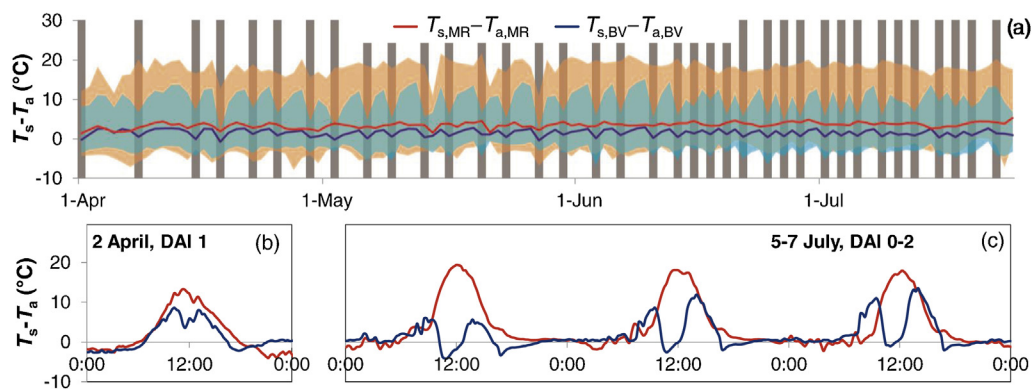


**Fig. 3.** Difference between soil surface and air temperature in the midrow ( $T_{s,MR}$  and  $T_{a,MR}$ ) and below the vine ( $T_{s,BV}$  and  $T_{a,BV}$ ) for the 2012 growing season. (a) average daily values, where shaded areas represent the range between daily maximum and minimum temperatures, and gray bars are days with irrigation, (b) and (c) diurnal patterns with 15 min resolution showing dynamics on different days after irrigation (DAI).

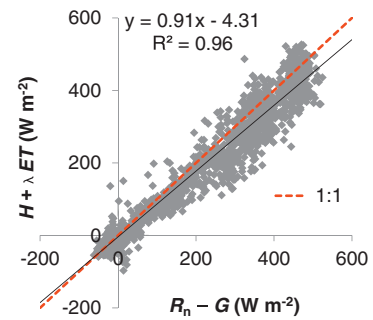


**Fig. 4.** Comparison of the sum of net radiation ( $R_n$ ) and soil heat flux ( $G$ ) to the sum of sensible and latent heat flux ( $H$  and  $\lambda ET$ , respectively).

#### 3.2.2. Diurnal course of the energy balance components

Instantaneous energy balance components at system level along with the midrow and below-vine positions are shown for a week in July when the canopy was fully developed (Fig. 5). System  $R_n$  (Fig. 5a) followed an invariable pattern reaching just below  $600 \text{ W m}^{-2}$  at noon, with no evidence of clouds. Below the canopy,  $R_{n,BV}$  (Fig. 5b) and  $R_{n,MR}$  (Fig. 5c) were similarly invariable from day to day reaching around  $400 \text{ W m}^{-2}$ . At the below-vine position  $R_{n,BV}$ , as well as  $G_{BV}$ ,  $H_{s,BV}$ , and  $\lambda E$ , were reduced strongly at midday due to shading by the canopy. In the midrow  $R_{n,MR}$  showed a plateau at midday, a phenomena that was not observed early in the season when  $R_{n,MR}$  resembled system  $R_n$ . System  $G$  was a weighted composite of  $G_{BV}$  and  $G_{MR}$  where  $G$  at both positions reached a maximum around  $160 \text{ W m}^{-2}$  and remained fairly constant from day to day. A slight reduction in  $G_{BV}$  was observed following irrigation events. System turbulent fluxes  $H$  and  $\lambda ET$  were similar in magnitude, reaching maximums between  $130$  and  $300 \text{ W m}^{-2}$ , where ratios between  $H$  and  $\lambda ET$  differed depending on the time passed since the last irrigation event. During a 3-day irrigation interval,  $\lambda ET$  was reduced by half on the second day following irrigation, and did not recover immediately when irrigation was applied the next day (Fig. 5, 15 July). Below the canopy, irrigation caused an immediate drop in  $H_{s,BV}$  reaching a maximum of  $64 \text{ W m}^{-2}$  on days of irrigation, increasing up to  $191 \text{ W m}^{-2}$  on the following day, and up to  $256 \text{ W m}^{-2}$  on the second day without irrigation. Midrow  $H_{s,MR}$  consistently reached a maximum between  $260$  and  $330 \text{ W m}^{-2}$ .

While below canopy instantaneous fluxes appeared to follow a reasonable pattern subject to diurnal shading and irrigation patterns, the response times of  $R_{ns}$ ,  $G$ , and  $H_s$  to quickly changing light intensities did not appear to be uniform. A sketch of below canopy shading (Fig. 6) demonstrates that for specific times within

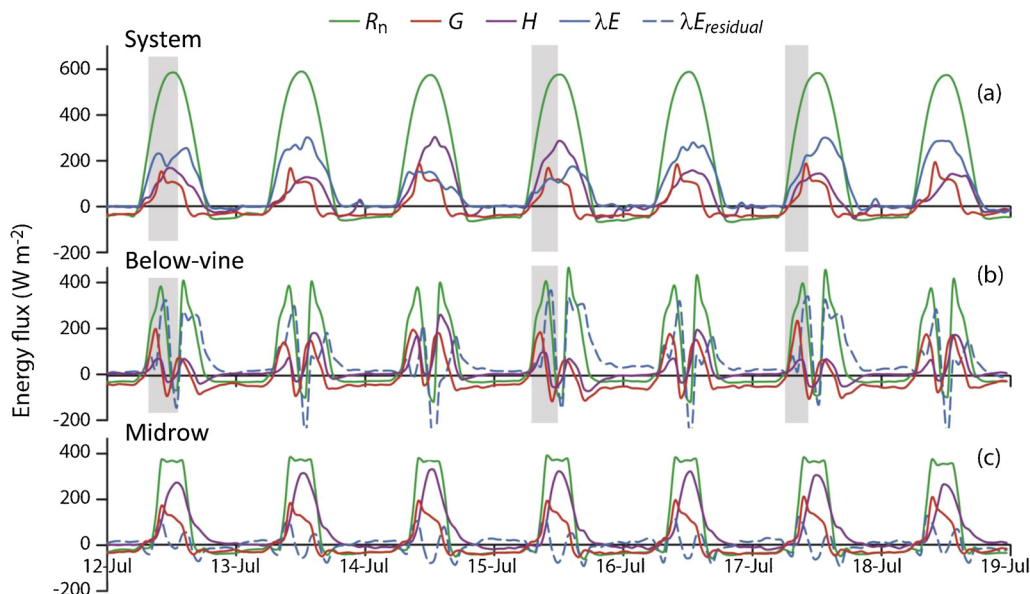


**Fig. 5.** Energy balance components  $R_n$  (net radiation),  $G$  (soil heat flux),  $H$  (sensible heat flux), and  $\lambda E$  (latent heat flux), at system level (a) and below the canopy at below-vine (b) and midrow (c) positions, where below canopy  $\lambda E$  is the residual of the instantaneous fluxes. Gray bars indicate irrigation.

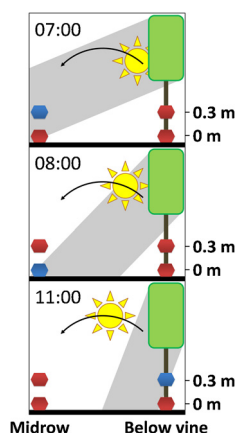


**Fig. 6.** Shade experienced at measurement locations in the midrow and directly below the vine, where blue is shaded and red is sunlit. Subscripts denote height in m above the surface. (For interpretation of the references to color in this figure legend, the reader is referred to the web version of this article.)

the day the shading was not uniform at all below vine measurement heights at a given horizontal positions. In other words, there were times, for instance, when the soil was shaded but the same position 30 cm above the ground was sunlit. Thus, the net radiation represented sunlit conditions while the soil heat flux represented shaded conditions. The shading patterns shown in Fig. 6 were visible in the afternoon but in reverse order. Because  $\lambda E$  was computed as the residual of the respective energy balance components this resulted in uncertainty in  $\lambda E$  estimates, particularly in the early morning and late evening in the midrow, and the period around noon at the below-vine position. This is evident in Fig. 5, where  $\lambda E$  computed as the residual of the instantaneous fluxes in the midrow summed to zero on a daily basis but peaked around sunrise and sunset. Similarly  $\lambda E$  computed as the residual of the instantaneous fluxes at the below-vine position may not be reliable around noon. Further analyses of energy and evapotranspiration partitioning were therefore done for daily time intervals, where daily  $\lambda E$  was computed as the residual of the daily sums of  $R_{ns,BV}$ ,  $H_{s,BV}$  and  $G_{BV}$ .

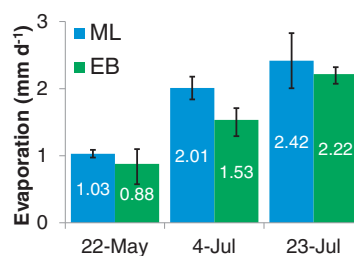


**Fig. 7.** Micro-lysimeter (ML;  $n = 2$  for 22 May and 4 July and  $n = 6$  for 23 July) versus energy balance (EB)-based evaporation estimates for the area directly below the vine (2012). EB error bars represent calculations using upper and lower limits of midrow air temperature.

### 3.2.3. Validation of computed daily E

A 24-h comparison was made between  $E$  computed from the energy balance and  $E$  measured with the MLs for three different days during the season (Fig. 7).

Both  $E$  rates represent an average for the below-vine position. The ML measurements are an average of drier and wetter positions along the drip line, while energy balance  $E$  rates are shown as calculated for the below-vine position, prior to applying the 14% scaling factor. The upper limit of  $E$  rates as computed by the energy balance occurs when  $T_{a,MR} = T_{ac}$ , while the lower limit is for  $T_{a,MR} = [(1 - 0.3)T_{ac} + 0.3T_{s,MR}]$ . Results were very similar for 22 May, which was two days after irrigation. On 4 and 23 July, both one day after irrigation, energy balance  $E$  values were lower. Average energy balance  $E$  values underestimated average ML derived values by 8–24%, or 16% on average.

## 3.3. Seasonal energy and evapotranspiration partitioning

### 3.3.1. Energy partitioning

Seasonal partitioning of  $R_n$  into  $G$ ,  $H$ , and  $\lambda ET$  (or  $R_{ns}$ ,  $H_s$  and  $\lambda E$  below the canopy) was assessed for the system and for the two positions below the canopy, midrow and below-vine (Fig. 8). Average system  $R_n$  increased from 9.36 MJ m<sup>-2</sup> d<sup>-1</sup> in April to 15.13 MJ m<sup>-2</sup> d<sup>-1</sup> in July. Seasonal average below canopy  $R_{ns,BV}$  and  $R_{ns,MR}$  were  $5.41 \pm 0.77$  MJ m<sup>-2</sup> d<sup>-1</sup> and  $5.91 \pm 0.81$  MJ m<sup>-2</sup> d<sup>-1</sup>, respectively, without showing a clear trend. Dust storms on 18 and

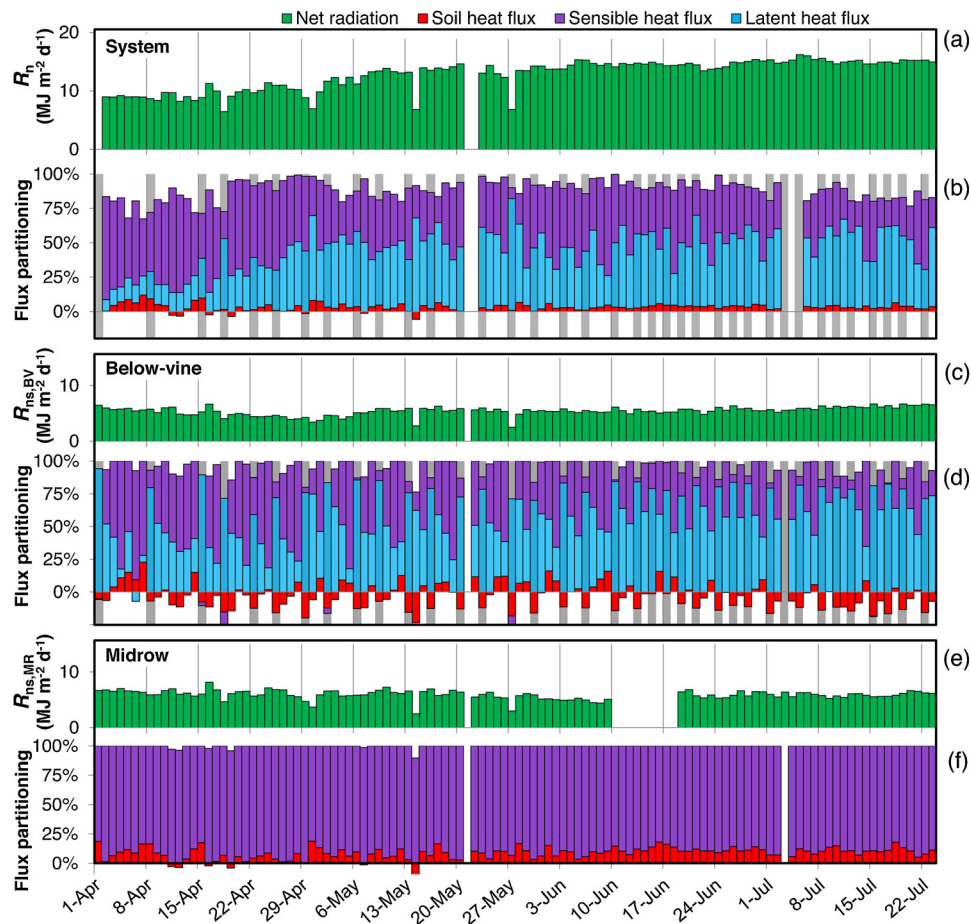


**Fig. 8.** Energy partitioning at system level and below the canopy at the below-vine and midrow positions. Net radiation ( $R_n$ ) is the sum of soil, sensible and latent heat flux at system, below-vine ( $R_{ns,BV}$ ), and midrow ( $R_{ns,MR}$ ) positions. Gray bars in panels (b) and (d) indicate irrigation.

30 April and on 14 and 17 May caused up to 50% reduction in  $R_n$  compared to other days around the same time.

For the whole season, system  $G$  was 3% of  $R_n$ , while  $H$  and  $\lambda ET$  were about equal amounting to 42% and 44% of  $R_n$ , respectively. During the first two weeks of the season, when irrigation was applied once a week and the canopy was just starting to develop,  $H$  was 60% and  $\lambda ET$  14%. Irrigation was applied bi-weekly from 15 April to 15 June during which  $H$  was 45%,  $\lambda ET$  44%, and  $G$  3%, similar to the seasonal average. Toward the summer (June 15) irrigation was increased to tri-weekly and the  $\lambda ET$  fraction increased to 48%,  $H$  reduced to 36% and  $G$  was 4%. At the below-vine position seasonal sums of  $\lambda E$  and  $H_{s,BV}$  amounted to 67% and 38% of  $R_{ns,BV}$ , respectively, while  $G_{BV}$  was negative with  $-5\%$ .  $G_{BV}$  showed a strong response to irrigation, amounting to an average of  $-18\%$  of  $R_{ns,BV}$  on irrigated days,  $-5\%$  on first days after irrigation and 6% on following days. The irrigated days, first days after irrigation, and following days each comprised about one third of the total number of days studied. On irrigated days,  $\lambda E$  was 110% of  $R_{ns,BV}$ , decreasing to 63% on the following day and 31% after two or more days. Average  $H_{s,BV}$  was much lower with 8% of  $R_{ns,BV}$  on irrigated days, increasing to 41% after one day and 63% after two or more days. In the midrow, seasonal average  $H_{s,MR}$  was 92% and  $G_{MR}$  equaled 8%. Early in the season a somewhat lower  $G_{MR}$  appeared to coincide with more erratic weather patterns.

### 3.3.2. Evapotranspiration partitioning

Comparison of seasonal  $E$  versus  $ET$  is shown in Fig. 9, where  $ET_0$  is given as a reference of weather conditions. Average  $ET_0$  increased from  $6.21 \text{ mm d}^{-1}$  in April to  $7.7 \text{ mm d}^{-1}$  in June and July. Patterns

of increasing  $ET$  resembled those of LAI, while  $E$  remained relatively stable throughout the season. During the second part of the season, after the canopy was fully developed, maximum  $ET$  was around  $3.5 \text{ mm d}^{-1}$ , occurring either on the day of, or on the day following irrigation. A strong decrease in  $ET$  was observed at the end of longer irrigation intervals, with values of about  $2 \text{ mm d}^{-1}$ . Total  $E$  was  $0.35 \pm 0.06 \text{ mm d}^{-1}$  on days with irrigation,  $0.19 \pm 0.05 \text{ mm d}^{-1}$  on the day after, and  $0.10 \pm 0.04 \text{ mm d}^{-1}$  on following days. Seasonal  $ET$  partitioning was determined by subtracting  $E$  from  $ET$ .

Development of  $K_c$  and  $K_{cb}$  over time was estimated by fitting a sigmoidal curve to  $ET/ET_0$  and  $T/ET_0$  for days that represented well-watered conditions (Fig. 10). As the highest values of  $T/ET_0$  generally occurred one day after irrigation (DAI 1) rather than on DAI 0, and  $K_{cb}$  was the primary contributor to  $K_c$ , both  $K_c$  and  $K_{cb}$  curves were fitted to DAI 1. At full canopy,  $K_c$  was 0.45 and  $K_{cb}$  was 0.42. In contrast, values of  $E/ET_0$  were clearly highest on DAI 0, averaging about 0.05 and reducing to 0.03 and 0.01 on DAI 1 and DAI >1, respectively. Values for  $E/ET_0$  appeared to remain constant throughout the season.

Partitioning of  $ET$  showed that early in the season  $E$  was a relatively large fraction of  $ET$  (Fig. 11). Within a few weeks however,  $T$  dominated  $ET$ , reaching a cumulative 88% fraction by 3 May after which it comprised  $90 \pm 1\%$  of  $ET$ . Cumulative  $ET$  measured from bud break until harvest (April–July) was 261 mm, where  $E$  (=24 mm) was 9% of  $ET$ , and  $T$  (=237 mm) accounted for 91% of  $ET$  (Fig. 12). Difference between  $ET$  and irrigation reached a maximum on 23 June, after which it remained more or less constant, indicating depletion of pre-season accumulated soil water and commencing of irrigation as the only source of water for  $ET$ .

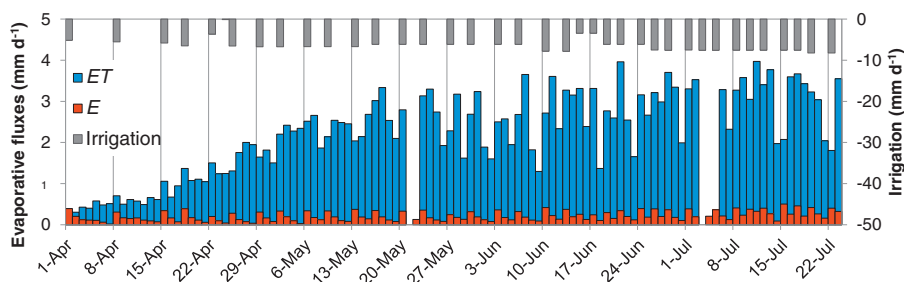


Fig. 9. Reference evapotranspiration ( $ET_0$ ), evapotranspiration ( $ET$ ) and soil water evaporation ( $E$ ) for the growing season of 2012.

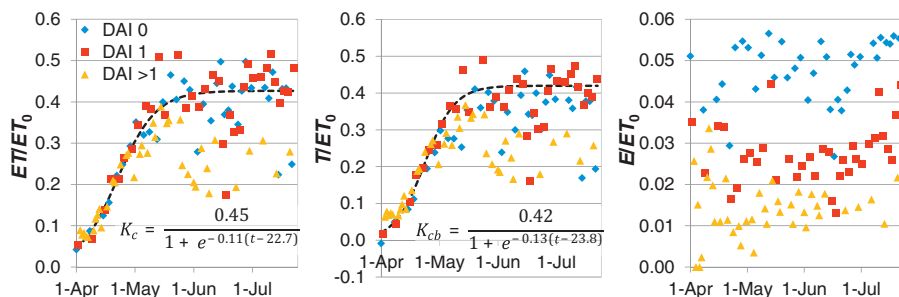


Fig. 10. Evapotranspiration ( $ET$ ), transpiration ( $T$ ), and soil water evaporation ( $E$ ) as a fraction of reference  $ET_0$  during the season of 2012. Daily values were plotted separately for 0, 1, or >1 day(s) after irrigation (DAI). A sigmoidal curve was fitted to well-watered days to represent crop coefficients for  $ET$  ( $K_c$ ) and  $T$  ( $K_{cb}$ ), where  $t$  is time in days since bud break.

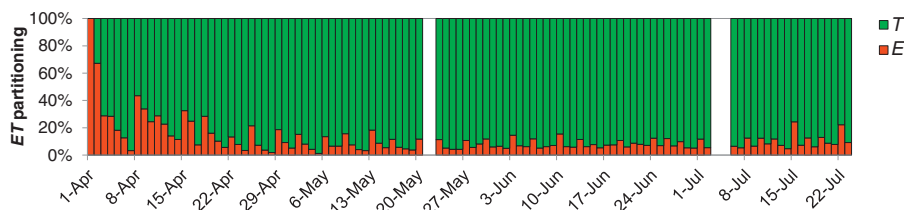


Fig. 11. Evapotranspiration ( $ET$ ) partitioning into transpiration ( $T$ ) and evaporation ( $E$ ) for the growing season of 2012.

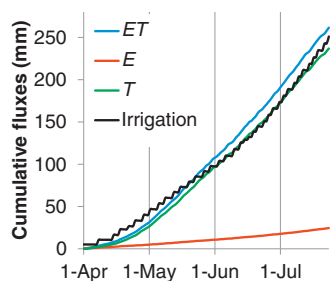


Fig. 12. Cumulative evapotranspiration ( $ET$ ), evaporation from the soil ( $E$ ) and transpiration ( $T$ ) fluxes for season 2012.

#### 4. Discussion

Weather conditions as well as canopy development in the vineyard were stable from the end of May through July, making irrigation the major source of variability in energy and evaporation fluxes for the main part of the season. Values for LAI were similar to those reported for Cabernet Sauvignon in other areas of the Negev desert in Israel (Cohen et al., 2000). The lack of major changes in  $F_{VA}$  over the season, indicates that the seasonal trends were adequately described by the original formulation.

Other resistance formulations were considered for  $r_{as}$ , including an approach that assumes the below canopy  $r_{as}$  is equivalent to that for a bare soil (Horton, 1989; Evett and Lascano, 1993;

Qiu et al., 1999) and an approach for sparse crops (Shuttleworth and Gurney, 1990; Shuttleworth and Wallace, 1985) used by Ham and Heilman (1991) and Nichols (1992). The current approach was adopted because it resulted in the highest  $R^2$  and lowest RMSE in the optimization of  $H$  below the canopy. This indicates the importance of including  $[T_s - T_a]$  in the computation of  $r_{as}$ , one of the key differences between this formulation and the other approaches. Further investigation is necessary to determine the physical meaning of  $F_{VA}$  or to improve estimation of  $u_s$  for vineyard architecture.

As expected, surface wetness and shading patterns caused  $T_s$  to be different at below-vine and midrow positions, highlighting the importance of assessing the dry bare midrow and the wetter areas near the dripper directly underneath the vine independently. At the below-vine position,  $T_s$  dropped below  $T_a$  at noon, producing a marked contrast with the midrow. Similar magnitudes of  $[T_s - T_a]$  were found by Hicks (1973), who reported  $[T_s - T_a]$  reached 25 °C. Surprisingly, similar magnitudes of  $[T_s - T_a]$  values were maintained throughout the growing season.

System energy balance closure of 0.88 was relatively good, considering that average energy imbalance at FLUXNET sites is 20% (Wilson et al., 2002). Since  $\lambda ET$  was more or less equal to irrigation for the latter part of the season (Fig. 12), the values for  $\lambda ET$  were considered reliable.

Daily peak system  $R_n$  was comparable to values reported in other vineyards (Heilman et al., 1994; Ortega-Farías et al., 2007; Shapland et al., 2012; Trambouze et al., 1998). The similarity between above and below  $R_n$  early on in the season has been found elsewhere

(Heilman et al., 1994), while mid- and late-season differences between above and below canopy  $R_n$  (Fig. 5) resemble findings by Pieri (2010a). Maximum values of  $G$  were in the range of  $50 \text{ W m}^{-2}$  and  $254 \text{ W m}^{-2}$  reported for vineyards by Trambouze et al. (1998) and Heilman et al. (1994). Similar to Heilman et al. (1994), peak values of  $G$  occurred in the morning, and, as suggested by Monteith and Unsworth (2008), the time difference between peak surface temperature and peak  $G$  was about 3 h.

The strong effect of irrigation on  $H$  and  $\lambda ET$  is different from the slightly higher and generally constant values reported for a rain-fed vineyard by Trambouze et al. (1998). The more abrupt changes may be a product of the relatively small wetted soil volume that is characteristic for drip irrigated systems. This gives vine roots very little buffer when the soil dries out, as is apparent from the sudden drop in  $\lambda ET$  after only two days without irrigation and the subsequent lag in recovery following the next irrigation (Fig. 5). Below canopy energy fluxes have been reported for a flood-irrigated vineyard in Texas (Heilman et al., 1994) where maximum values of  $205 \text{ W m}^{-2}$  for  $\lambda E$  were similar to values found at the below-vine position near the dripper, while maximum  $H_s$  ( $254 \text{ W m}^{-2}$ ) was between flux values for midrow and below-vine observations in our system. However, differences in irrigation, and lack of measurements at the below-vine position where shading affects fluxes most strongly, limited further comparison.

An evaluation of change in below-canopy  $R_{ns}$  with height above the surface, using models, showed that  $R_{ns}$  measurements at the lowest possible height are not representative of instantaneous fluxes at the soil surface (Pieri, 2010b). It appears therefore that the computation of instantaneous  $\lambda E$  as the residual of the below canopy energy balance may not be possible using conventional measurements of  $R_{ns}$ . However, daily averages at  $0.27 \text{ m}$  height did accurately represented daily  $R_{ns}$  fluxes at the surface (Pieri, 2010b). Comparison of energy balance  $E$  with ML measurements suggests that  $E$  may be somewhat underestimated. This may indicate that  $T_{a,MR}$  is closer to  $T_{ac}$  than to  $[(1 - 0.3)T_{ac} + 0.3 T_{s,MR}]$ . However, even for  $T_{a,MR} = T_{ac}$  the values appear to be on the low side for the first day after irrigation (4 and 23 July), suggesting that total energy available for  $\lambda E$  was underestimated, perhaps due to advection from the midrow. Considering that the temperature gradient between the surface of the midrow and the below-vine position decreased with time after irrigation (see Section 3.1.2), this effect would be less on the second day following irrigation. An average seasonal bias of 16% would increase the computed percentage of  $E$  relative to  $ET$  by 2%.

Seasonal energy balance partitioning showed that for 6 or 7 weeks following bud break,  $R_n$  varied little; reaching fluxes similar to late season fluxes of  $14 \text{ MJ m}^{-2} \text{ d}^{-1}$  reported by Shapland et al. (2012), and  $11\text{--}16 \text{ MJ m}^{-2} \text{ d}^{-1}$  reported by Yunusa et al. (2004). For a variety of vineyards,  $R_n$  was reported to partition into 2–11%  $G$ , 38–59%  $H$ , and 37–51%  $\lambda ET$  (Shapland et al., 2012; Trambouze et al., 1998; Yunusa et al., 2004; Zhang et al., 2007). In comparison, measured  $\lambda ET$  at full canopy was on the high side, while  $H$  and  $G$  were on the low side. For the early season, the first month after bud break, Zhang et al. (2007) reported much higher  $\lambda ET$  fractions compared to those found in the current study, however, the reverse was true the two months before harvest. Fractions of  $H$  and  $G$  were similar, however, with slightly higher fractions of  $G$  early in the season compared to later in the season.

Both below-vine and midrow positions did not show much variation in  $R_{ns}$  over the season, even though  $R_n$  above the canopy increased by more than 50%. This can be attributed to the canopy serving as a sink for  $R_n$ , thus reducing the available energy at the soil surface. It appears that below the canopy, the increase in  $R_n$  going into summer observed at the system level was canceled out by canopy growth.

While the energy balance partitioning in the midrow was fairly consistent, the below-vine energy balance was regulated by irrigation events, with the relative fraction of  $\lambda E$  over the season increasing according to increases in irrigation frequency. If advection from the midrow occurs at times immediately following irrigation, as suggested by comparisons with ML data,  $\lambda E$  would be the sum of  $R_{ns,BV}$  and the advected energy. Average  $G_{BV}$  was negative over the season, indicating that the soil contributed to the available energy, in spite of the fact that the soil warmed over time (see Section 3.1.2). This suggests lateral heat flow from the midrow to the below-vine position, which is reasonable considering that total system  $G$  is positive and the large difference in surface temperature between the midrow and below-vine positions. A rough estimate of the lateral heat fluxes using surface temperature and an estimated thermal conductivity (data not shown) further confirmed that the deficit in  $G_{BV}$  could be explained by lateral heat fluxes. It should be noted that there is uncertainty in the magnitude of this deficit due to known errors in using heat flux plates in rapidly drying soil conditions (Ochsner et al., 2006; Sauer et al., 2003).

Seasonal  $ET_0$  values were relatively high compared to other vineyard sites, though daily  $ET$  values were quite similar (Kerridge et al., 2013; Poblete-Echeverría et al., 2012; Shapland et al., 2012; Yunusa et al., 2004; Zhang et al., 2007). Trambouze et al. (1998), for example, showed similar  $ET$  values of  $2.1\text{--}3.5 \text{ mm d}^{-1}$  for an average  $ET_0$  of about  $5.7 \text{ mm d}^{-1}$  during the months of June and July. In contrast, total  $E$  was quite low, mainly because the wetted area represented a very small fraction of the total vineyard surface area. The location of the drippers directly below the vine where shading at noon caused strong reduction in available energy, as well as the complete absence of rain, also contributed to relatively low total  $E$ .

The relation of seasonal  $K_{cb}$  to both LAI and  $f_{veg}$  was compared to six empirical formulations reported in the literature (Ferreira et al., 2012; Picón-Toro et al., 2012; Williams and Ayars, 2005). The LAI and  $f_{veg}$  were on the lower end of the calibrations reported, resulting in a lower  $K_{cb}$ . This is consistent with the finding mentioned earlier, that  $ET_0$  is higher than average while  $ET$  is similar to other studies. Five of the formulations gave a reasonable result with maximum  $f_{veg}$  and LAI resulting in  $K_{cb}$  values of 0.39–0.43. The one exception was a  $K_{cb}$  of 0.28 using the  $f_{veg}$  equation of Williams and Ayars (2005); even though their equation using LAI gave a reasonable estimate with a  $K_{cb}$  of 0.43. This may be explained by the fact that they studied table grapes where the canopy is much less clumped. When considering the whole study period, however, all equations overestimated  $K_{cb}$  by 30–50% for lower LAI and  $f_{veg}$  values. Relationships determined for this study were:  $[K_{cb} = 0.011 \times f_{veg} + 0.249]$  and  $[K_{cb} = 0.129 \times \text{LAI} + 0.249]$ . This may indicate that relations between  $K_{cb}$  and plant size parameters are more universal for fully grown canopies. Non-universality of  $K_c$  factors can also be ascribed to the site-specific nature of the wind fitting terms that relate  $K_c$  to  $ET_0$  (Allen et al., 1998). Additionally, the significant scatter observed in Fig. 11 for the actual  $K_{cb}$  and  $K_c$  values as both plateau at peak vine cover indicates there is large day-to-day uncertainty in crop coefficients applied to vineyards.

Average  $E/ET$  and  $T/ET$  previously reported for vineyards were  $0.41 \pm 0.21$  and  $0.57 \pm 0.21$ , respectively (Kool et al., 2014a). For drip-irrigated vineyards, reported  $E/ET$  and  $T/ET$  averaged  $0.30 \pm 0.12$  and  $0.69 \pm 0.13$  (Ferreira et al., 2012; Kerridge et al., 2013; Poblete-Echeverría et al., 2012; Yunusa et al., 2004). In comparison, water use of the vineyard in this study was extremely efficient with an  $E/ET$  of only 9%, or 11% if a 16% underestimation of  $E$  is considered. It should be noted that the  $E/ET$  ratio is likely to increase post-harvest, during canopy senescence, when transpiration declines but irrigation continues.

## 5. Conclusion

The below canopy energy balance approach used in this study allowed continuous assessment of  $E$  at daily intervals, instantaneous  $\lambda E$  fluxes could not be assessed due to vertical variability in shading below the canopy. Seasonal (bud break to harvest)  $ET$  partitioning indicated total  $E$  amounted to 9–11% of  $ET$ , while  $K_c$  and  $K_{cb}$  were determined to reach 0.45 and 0.42, respectively, but had significant day-to-day variation. In the computation of below canopy energy fluxes, parameterization of wind speed proved to be most challenging.

Future challenges include a better formulation for soil surface aerodynamic resistance which does not require a calibration factor like  $F_{VA}$ . This is likely to require a better characterization of wind profiles in raised canopies common in viticulture. Additionally, energy partitioning needs to be assessed in relation to grape yield and wine quality. Further exploration of the below canopy energy balance approach may also be beneficial in other sparsely vegetated sites, specifically in studies already measuring surface temperatures of above and below canopy elements.

## Acknowledgments

This research was supported by Research Grant No. US-4262-09 from BARD, the United States–Israel Binational Agricultural Research and Development Fund, and was partially supported by the I-CORE Program of the Planning and Budgeting Committee and the Israel Science Foundation (grant no. 152/11). We are particularly grateful for technical and field support from the Gilat Research Center's Eugene Presnov and the Jacob Blaustein Institutes for Desert Research's Yuval Shani. We also thank Yoav Rabani for graciously providing his vineyard as an experimental site.

## References

- Allen, R.G., Pereira, L.S., Raes, D., Smith, M., 1998. *Crop Evapotranspiration-Guidelines for Computing Crop Water Requirements*, FAO—Food and Agriculture Organization of the United, FAO, Rome.
- Castellví, F., Snyder, R.L., 2009. Sensible heat flux estimates using surface renewal analysis. *Agric. For. Meteorol.* 149, 1397–1402, <http://dx.doi.org/10.1016/j.agrformet.2009.03.011>.
- Choudhury, B.J., Monteith, J.L., 1988. A four-layer model for the heat budget of homogeneous land surfaces. *Q. J. R. Meteorol. Soc.* 114, 373–398.
- Cohen, S., Striem, M.J., Bruner, M., Klein, I., 2000. Grapevine leaf area index evaluation by gap fraction inversion. *Acta Hort.* 567, 87–94, <http://dx.doi.org/10.17660/ActaHortic.2000.537.7>.
- Colaizzi, P.D., Kustas, W.P., Anderson, M.C., Agam, N., Tolch, J.A., Evett, S.R., Howell, T.A., Gowda, P.H., O'Shaughnessy, S.A., 2012. Two-source energy balance model estimates of evapotranspiration using component and composite surface temperatures. *Adv. Water Resour.* 50, 134–151, <http://dx.doi.org/10.1016/j.advwatres.2012.06.004>.
- Ding, R., Kang, S., Zhang, Y., Hao, X., Tong, L., Li, S., 2015. A dynamic surface conductance to predict crop water use from partial to full canopy cover. *Agric. Water Manage.* 150, 1–8, <http://dx.doi.org/10.1016/j.agwat.2014.11.010>.
- Evett, S.R., Lascano, R.J., 1993. ENWATBAL.BAS: a mechanistic evapotranspiration model written in compiled BASIC. *Agron. J.* 85, 763–772.
- Ferreira, M.I., Silvestre, J., Conceição, N., Malheiro, A.C., 2012. Crop and stress coefficients in rainfed and deficit irrigation vineyards using sap flow techniques. *Irrig. Sci.* 30, 433–447, <http://dx.doi.org/10.1007/s00271-012-0352-2>.
- Fratini, G., McDermitt, D.K., Papale, D., 2014. Eddy-covariance flux errors due to biases in gas concentration measurements: origins, quantification and correction. *Biogeosciences* 11, 1037–1051, <http://dx.doi.org/10.5194/bg-11-1037-2014>.
- Goring, D.G., Nikora, V.I., 2002. Despiking acoustic doppler velocimeter data. *J. Hydraul. Eng.* 128, 117–126.
- Goudriaan, J., 1977. *Crop Micrometeorology: A Simulation Study (Simulation Monographs)*. Pudoc, Center for Agricultural Publishing and Documentation, Wageningen.
- Ham, J.M., Heilman, J.L., 1991. Aerodynamic and surface resistances affecting energy transport in a sparse crop. *Agric. For. Meteorol.* 53, 267–284.
- Heilman, J.L., McInnes, K., Savage, M., Gesch, R., Lascano, R.J., 1994. Soil and canopy energy balances in a west Texas vineyard. *Agric. For. Meteorol.* 71, 99–114, [http://dx.doi.org/10.1016/0168-1923\(94\)90102-3](http://dx.doi.org/10.1016/0168-1923(94)90102-3).
- Hicks, B.B., 1973. Eddy fluxes over a vineyard. *Agric. Meteorol.* 12, 203–215, [http://dx.doi.org/10.1016/0002-1571\(73\)90020-4](http://dx.doi.org/10.1016/0002-1571(73)90020-4).
- Horton, R., 1989. Canopy shading effects on soil heat and water flow. *Soil Sci. Soc. Am. J.* 53, 669–679.
- Horton, R., Aguirre-Luna, O., Wierenga, P.J., 1984. Soil temperature in a row crop with incomplete surface cover. *Soil Sci. Soc. Am. J.* 48, 1225–1232.
- Kerridge, B.L., Hornbuckle, J.W., Christen, E.W., Faulkner, R.D., 2013. Using soil surface temperature to assess soil evaporation in a drip irrigated vineyard. *Agric. Water Manage.* 116, 128–141, <http://dx.doi.org/10.1016/j.agwat.2012.07.001>.
- Kool, D., Agam, N., Lazarovitch, N., Heitman, J.L., Sauer, T.J., Ben-Gal, A., 2014a. A review of approaches for evapotranspiration partitioning. *Agric. For. Meteorol.* 184, 56–70, <http://dx.doi.org/10.1016/j.agrformet.2013.09.003>.
- Kool, D., Ben-Gal, A., Agam, N., Šimúnek, J., Heitman, J.L., Sauer, T.J., Lazarovitch, N., 2014b. Spatial and diurnal below canopy evaporation in a desert vineyard: measurements and modeling. *Water Resour. Res.* 50, 7035–7049, <http://dx.doi.org/10.1002/2014WR015409>.
- Kustas, W.P., Norman, J.M., 1999. Evaluation of soil and vegetation heat flux predictions using a simple two-source model with radiometric temperatures for partial canopy cover. *Agric. For. Meteorol.* 94, 13–29, [http://dx.doi.org/10.1016/S0168-1923\(99\)00005-2](http://dx.doi.org/10.1016/S0168-1923(99)00005-2).
- Lawrence, D.M., Thornton, P.E., Oleson, K.W., Bonan, G.B., 2007. The partitioning of evapotranspiration into transpiration, soil evaporation, and canopy evaporation in a GCM: impacts on land–atmosphere interaction. *J. Hydrometeorol.* 8, 862–880, <http://dx.doi.org/10.1175/JHM596.1>.
- Li, S., Tong, L., Li, F., Zhang, L., Zhang, B., Kang, S., 2009. Variability in energy partitioning and resistance parameters for a vineyard in northwest China. *Agric. Water Manage.* 96, 955–962, <http://dx.doi.org/10.1016/j.agwat.2009.01.006>.
- Liu, H., Peters, G., Foken, T., 2001. New equations for sonic temperature variance and buoyancy heat flux with an omnidirectional sonic anemometer. *Boundary Layer Meteorol.* 100, 459–468.
- Massman, W.J., 2000. A simple method for estimating frequency response corrections for eddy covariance systems. *Agric. For. Meteorol.* 104, 185–198, [http://dx.doi.org/10.1016/S0168-1923\(00\)00164-7](http://dx.doi.org/10.1016/S0168-1923(00)00164-7).
- Monteith, J.L., Unsworth, M.H., 2008. *Principles of Environmental Physics*, third ed. Elsevier/Academic Press, Burlington, MA.
- Netzer, Y., Yao, C., Shenker, M., Bravdo, B.-A., Schwartz, A., 2009. Water use and the development of seasonal crop coefficients for Superior Seedless grapevines trained to an open-gable trellis system. *Irrig. Sci.* 27, 109–120, <http://dx.doi.org/10.1007/s00271-008-0124-1>.
- Nichols, W.D., 1992. Energy budgets and resistances to energy transport in sparsely vegetated rangeland. *Agric. For. Meteorol.* 60, 221–247.
- Norman, J.M., Kustas, W.P., Humes, K.S., 1995. Source approach for estimating soil and vegetation energy fluxes in observations of directional radiometric surface temperature. *Agric. For. Meteorol.* 77, 263–293, [http://dx.doi.org/10.1016/0168-1923\(95\)02265-Y](http://dx.doi.org/10.1016/0168-1923(95)02265-Y).
- Ochsner, T.E., Sauer, T.J., Horton, R., 2006. Field tests of the soil heat flux plate method and some alternatives. *Agron. J.* 98, 1005–1014, <http://dx.doi.org/10.2134/agronj2005.0249>.
- Ortega-Farías, S., Carrasco, M., Olioso, A., Acevedo, C., Poblete, C., 2007. Latent heat flux over Cabernet Sauvignon vineyard using the Shuttleworth and Wallace model. *Irrig. Sci.* 25, 161–170, <http://dx.doi.org/10.1007/s00271-006-0047-7>.
- Ortega-Farías, S., Poblete-Echeverría, C., Brisson, N., 2010. Parameterization of a two-layer model for estimating vineyard evapotranspiration using meteorological measurements. *Agric. For. Meteorol.* 150, 276–286, <http://dx.doi.org/10.1016/j.agrformet.2009.11.012>.
- Picón-Toro, J., González-Dugo, V., Uriarte, D., Mancha, L.A., Testi, L., 2012. Effects of canopy size and water stress over the crop coefficient of a “Tempranillo” vineyard in south-western Spain. *Irrig. Sci.* 30, 419–432, <http://dx.doi.org/10.1007/s00271-012-0351-3>.
- Pieri, P., 2010a. Modelling radiative balance in a row-crop canopy—cross-row distribution of net radiation at the soil surface and energy available to clusters in a vineyard. *Ecol. Modell.* 221, 802–811, <http://dx.doi.org/10.1016/j.ecolmodel.2009.07.028>.
- Pieri, P., 2010b. Modelling radiative balance in a row-crop canopy: row-soil surface net radiation partition. *Ecol. Modell.* 221, 791–801, <http://dx.doi.org/10.1016/j.ecolmodel.2009.11.019>.
- Poblete-Echeverría, C., Ortega-Farías, S., 2009. Estimation of actual evapotranspiration for a drip-irrigated Merlot vineyard using a three-source model. *Irrig. Sci.* 28, 65–78, <http://dx.doi.org/10.1007/s00271-009-0183-y>.
- Poblete-Echeverría, C., Ortega-Farías, S., Zuñiga, M., Fuentes, S., 2012. Evaluation of compensated heat-pulse velocity method to determine vine transpiration using combined measurements of eddy covariance system and microlysimeters. *Agric. Water Manage.* 109, 11–19, <http://dx.doi.org/10.1016/j.agwat.2012.01.019>.
- Qiu, G.Y., Momii, K., Yano, T., Lascano, R.J., 1999. Experimental verification of a mechanistic model to partition evapotranspiration into soil water and plant evaporation. *Agric. For. Meteorol.* 93, 79–93.
- Raupach, M.R., 1992. Drag and drag partition on rough surfaces. *Boundary Layer Meteorol.* 60, 375–395, <http://dx.doi.org/10.1007/BF00155203>.
- Riou, C., Pieri, P., Valancogne, C., 1987. Variation de la vitesse du vent a l'intérieur et au-dessus d'une vigne. *Agric. For. Meteorol.* 39, 143–154, [http://dx.doi.org/10.1016/0168-1923\(87\)90033-5](http://dx.doi.org/10.1016/0168-1923(87)90033-5).

- Sauer, T.J., 2002. Heat flux density. In: Dane, J.D., Topp, G.C. (Eds.), *Methods of Soil Analysis—Part 1, Physical and Mineralogical Methods*. American Society of Agronomy, Madison, WI, pp. 1233–1248.
- Sauer, T.J., Meek, D.W., Ochsner, T.E., Harris, A.R., Horton, R., 2003. Errors in heat flux measurement by flux plates of contrasting design and thermal conductivity. *Vadose Zone J.* 2, 580–588, <http://dx.doi.org/10.2136/vzj2003.0580>.
- Schotanus, P., Nieuwstadt, F.T.M., De Bruin, H.A.R., 1983. Temperature measurement with a sonic anemometer and its application to heat and moisture fluxes. *Boundary Layer Meteorol.* 26, 81–93.
- Sene, K.J., 1994. Parameterisations for energy transfers from a sparse vine crop. *Agric. For. Meteorol.* 71, 1–18, [http://dx.doi.org/10.1016/0168-1923\(94\)90097-3](http://dx.doi.org/10.1016/0168-1923(94)90097-3).
- Shapland, T.M., Snyder, R.L., Smart, D.R., Williams, L.E., 2012. Estimation of actual evapotranspiration in winegrape vineyards located on hillside terrain using surface renewal analysis. *Irrig. Sci.* 30, 471–484, <http://dx.doi.org/10.1007/s00271-012-0377-6>.
- Shaw, R.H., 1977. Secondary wind speed maxima inside plant canopies. *J. Appl. Meteorol.* 16, 514–521, [http://dx.doi.org/10.1175/1520-0450\(1977\)016<0514:SWSMIP>2.0.CO;2](http://dx.doi.org/10.1175/1520-0450(1977)016<0514:SWSMIP>2.0.CO;2).
- Shaw, R.H., Pereira, A.R., 1982. Aerodynamic roughness of a plant canopy: a numerical experiment. *Agric. Meteorol.* 26, 51–65, [http://dx.doi.org/10.1016/0002-1571\(82\)90057-7](http://dx.doi.org/10.1016/0002-1571(82)90057-7).
- Shuttleworth, W.J., 1991. Evaporation models in hydrology. In: Schmugge, T.J., André, J.-C. (Eds.), *Land Surface Evaporation*. Springer, New York, NY, pp. 93–120, [http://dx.doi.org/10.1007/978-1-4612-3032-8\\_5](http://dx.doi.org/10.1007/978-1-4612-3032-8_5).
- Shuttleworth, W.J., Gurney, R.J., 1990. The theoretical relationship between foliage temperature and canopy resistance in sparse crops. *Q. J. R. Meteorol. Soc.* 116, 497–519.
- Shuttleworth, W.J., Wallace, J.S., 1985. Evaporation from sparse crops—an energy combination theory. *Q. J. R. Meteorol. Soc.* 111, 839–855, <http://dx.doi.org/10.1256/smsqj.46909>.
- Spano, D., Snyder, R.L., Duce, P., Paw, U.K.T., 2000. Estimating sensible and latent heat flux densities from grapevine canopies using surface renewal. *Agric. For. Meteorol.* 104, 171–183, [http://dx.doi.org/10.1016/S0168-1923\(00\)00167-2](http://dx.doi.org/10.1016/S0168-1923(00)00167-2).
- Tanner, C.B., Thurtell, G.W., 1969. Anemometer measurements of Reynolds stress and heat transport in the atmospheric surface layer department of soil science. In: *Research and Development Tech Report ECOM 66-G22-F to the US Army Electronics Command*. University of Wisconsin, Madison, WI.
- Trambouze, W., Bertuzzi, P., Voltz, M., 1998. Comparison of methods for estimating actual evapotranspiration in a row-cropped vineyard. *Agric. For. Meteorol.* 91, 193–208, [http://dx.doi.org/10.1016/S0168-1923\(98\)00072-0](http://dx.doi.org/10.1016/S0168-1923(98)00072-0).
- Van Leeuwen, C., Tregouat, O., Choné, X., Bois, B., Pernet, D., Gaudillère, J.-P., 2009. Vine water status is a key factor in grape ripening and vintage quality for red Bordeaux wine How can it be assessed for vineyard management purposes. *J. Int. Sci. Vigne Vin* 43, 121–134.
- Webb, E.K., Pearman, G.I., Leuning, R., 1980. Correction of flux measurements for density effects due to heat and water vapour transfer. *Q. J. R. Meteorol. Soc.* 106, 85–100, <http://dx.doi.org/10.1002/qj.49710644707>.
- Wilcox, B.P., Breshears, D.D., Seyfried, M.S., 2003. Rangelands water balance on. In: Stewart, B.A., Howell, T.A. (Eds.), *Encyclopedia of Water Science*. Marcel Dekker, Inc, New York, NY, pp. 791–794, <http://dx.doi.org/10.1081/E-EWS>.
- Williams, L.E., Ayars, J.E., 2005. Grapevine water use and the crop coefficient are linear functions of the shaded area measured beneath the canopy. *Agric. For. Meteorol.* 132, 201–211, <http://dx.doi.org/10.1016/j.agrformet.2005.07.010>.
- Wilson, K., Goldstein, A., Falge, E., Aubinet, M., Baldocchi, D., Berbigier, P., Bernhofer, C., Ceulemans, R., Dolman, H., Field, C., Grelle, A., Ibrom, A., Law, B.E., Kowalski, A., Meyers, T., Moncrieff, J., Monson, R., Oechel, W., Tenhunen, J., Valentini, R., Verma, S., 2002. Energy balance closure at FLUXNET sites. *Agric. For. Meteorol.* 113, 223–243, [http://dx.doi.org/10.1016/S0168-1923\(02\)00109-0](http://dx.doi.org/10.1016/S0168-1923(02)00109-0).
- Wullschleger, S.D., Meinzer, F.C., Vertessy, R.A., 1998. A review of whole-plant water use studies in trees. *Tree Physiol.* 18, 499–512.
- Yunusa, I.A.M., Walker, R.R., Lu, P., 2004. Evapotranspiration components from energy balance, sapflow and microlysimetry techniques for an irrigated vineyard in inland Australia. *Agric. For. Meteorol.* 127, 93–107, <http://dx.doi.org/10.1016/j.agrformet.2004.07.001>.
- Zhang, B.Z., Kang, S.Z., Zhang, L., Du, T.S., Li, S.E., Yang, X.Y., 2007. Estimation of seasonal crop water consumption in a vineyard using Bowen ratio-energy balance method. *Hydrol. Process.* 21, 3635–3641, <http://dx.doi.org/10.1002/hyp>.
- Zhang, Y., Kang, S., Ward, E.J., Ding, R., Zhang, X., Zheng, R., 2011. Evapotranspiration components determined by sap flow and microlysimetry techniques of a vineyard in northwest China: dynamics and influential factors. *Agric. Water Manage.* 98, 1207–1214, <http://dx.doi.org/10.1016/j.agwat.2011.03.006>.